



ELSEVIER

Contents lists available at ScienceDirect

Journal of Magnetism and Magnetic Materials

journal homepage: www.elsevier.com/locate/jmmm

Research articles

Study of magnetic and magneto-transport properties of nanocrystalline Nd_{0.5}Ca_{0.5}MnO₃ compound: Observation of large magnetoresistanceKalipada Das^{a,*}, Snehal Mandal^b, Dipak Mazumdar^b, Pintu Sen^c, I. Das^b^a Department of Physics, Seth Anandram Jaipuria College, 10, Raja Naba Krishna Street, Kolkata 700005, India^b CMP Division, Saha Institute of Nuclear Physics, HBNI, 1/AF-Bidhannagar, Kolkata 700 064, India^c Variable Energy Cyclotron Centre, HBNI, 1/AF-Bidhannagar, Kolkata 700064, India

ARTICLE INFO

Keywords:

Manganites
Magnetoresistance
Disorder

ABSTRACT

Magnetic and magneto-transport properties of nanocrystalline Nd_{0.5}Ca_{0.5}MnO₃ compound are presented. In contrast to its bulk counterparts, with modification of the magnetic ground state, large magnetoresistance appeared in the presence of comparatively lower magnetic field in nanocrystalline compound. Additionally, the magnetic field induced insulator-metal transition took place in nanocrystalline compound with negligible thermal hysteresis. From application perspectives, observation of the low field magnetoresistance in this compound may be important for several uses in magnetic field sensor related technology. Fundamentally, the influences of the ferromagnetic phase fraction as well as the induced ferromagnetic interaction in nanocrystalline samples on magnetic and magneto-transport properties were addressed.

1. Introduction

Magnetic and magnetoresistive properties in doped perovskite manganites having general formula R_{1-x}B_xMnO₃ (R-rare earth and B-bivalent ions) were extensively studied in the last two decades [1–12]. Strong correlation nature between the several degrees of freedom (i.e. charge, spin and lattice) in doped perovskite manganites formulate this field as an intriguing field of fore-front research. Moreover, depending upon the bivalent ion (B-ions) doping percentage (i.e. 'x') several stimulating properties appear in contrast to the undoped RMnO₃ compound. Among the numerous induced properties in doped manganites, colossal magnetoresistance (CMR) effect, metal–insulator transition, appearance of ferromagnetism, charge ordering (CO) and large magnetocaloric effect (MCE) have acquired most attention from fundamental as well as technological aspects [1–8,11,12]. After the discovery of the colossal magnetoresistance (CMR) effect in doped perovskite manganite compounds in 1994 by Jin et al. [13], almost all the bulk compounds were extensively studied in next few years. In contrast to that, in case of nanomaterials, comparatively a less effort was paid. Recently, an incredible attention is remunerated for the study of physical properties of nanostructure forms of manganites due to their marvelous responses [3–5,11,12]. Regarding the CMR effect, it is generally governed by the suppression of the spin fluctuation at the vicinity of paramagnetic to ferromagnetic transition [13]. However, in case of the phase separated systems, it is governed by the subtle balance

between the competing phases in the external magnetic field [11,14]. Another interesting property of the doped perovskite manganites is charge ordering (CO). It is almost a generic properties of manganites and appears near to the half doping concentration. Electrically, charge ordered compounds exhibit insulating nature with decreasing of the temperature. To transform such insulating ground state into metallic state, large value of the external magnetic field is required in general [15]. In contrast to the bulk counterparts, different nature was found in charge ordered nanoparticles. With reduction of the particle size, comparatively small field is required to melt the charge ordered state [16]. Theoretically, Dong et al. pointed out that the uncompensated, short range ordered surface spins in nanoparticles plays the key role to the destabilization of the charge ordered fraction in the core part [10,17]. This phase separation phenomena induced large change of magnetoresistance and magnetocaloric effect even in charge ordered nanoparticles [16,18,19]. It was also reported that with the reduction of the particle size, ferromagnetic response is dominated over the anti-ferromagnetic fraction systematically [16–19]. Compared to the study of particle size mediated ferromagnetic volume fraction change in charge ordered nanoparticles, a less effort was paid to study the evolution of the modification of the ferromagnetic interaction with particle size. Recently Sarkar et al. reported that the increasing surface pressure with reduction of the particle size prevents the charge order formation and corroborates the predominant ferromagnetism [20]. However, Zang et al. pointed out the enhancement of ferromagnetic interaction in

* Corresponding author.

E-mail address: kalipadadasphysics@gmail.com (K. Das).<https://doi.org/10.1016/j.jmmm.2020.166421>

Received 3 August 2019; Received in revised form 10 December 2019; Accepted 7 January 2020

Available online 11 January 2020

0304-8853/ © 2020 Elsevier B.V. All rights reserved.

nanoparticles due to the destruction of the long range co-linear arrangement of antiferromagnetic ordering [21]. In contrast to that alternative arguments were also proposed in case of nanoparticles of charge ordered antiferromagnetic $\text{Nd}_{0.5}\text{Ca}_{0.5}\text{MnO}_3$ compound [22]. According to Zhou et al., with increasing ferromagnetic volume fraction in nanoparticles, the interaction strength of the ferromagnetic ordering also gets reduced [22]. The modifications in the magnetic properties due to the different contributing components in charge ordered nanoparticles have been extensively reported in several studies [1–10]. However, the influence of those parameters in magneto-transport properties is still the subject of intense debate. To address this issue we have considered the nanoparticles of $\text{Nd}_{0.5}\text{Ca}_{0.5}\text{MnO}_3$ compound having two different particle size which are ~ 38 nm (Nano-1) and ~ 56 nm (Nano-2).

Our experimental findings indicate that modification of the particle size induced ferromagnetic interaction remarkably influences the magneto-resistive properties of charge ordered $\text{Nd}_{0.5}\text{Ca}_{0.5}\text{MnO}_3$ nanoparticles from the fundamental point of view. Additionally, the observation of significantly large magnetoresistance in the $\text{Nd}_{0.5}\text{Ca}_{0.5}\text{MnO}_3$ nanoparticles may be important from several application perspectives.

2. Sample preparation and characterization:

$\text{Nd}_{0.5}\text{Ca}_{0.5}\text{MnO}_3$ nanoparticles were prepared by the sol-gel route. The constituent elements Nd_2O_3 , CaCO_3 and MnO_2 (pre-heated) were used for the sample preparation (99.9 % purity). To prepare the homogeneous solution, the oxides were converted to their nitrates form by adding concentrated nitric acid and dissolved in millipore water individually. Special attention was taken for the MnO_2 as it does not dissolve directly in nitric acid. MnO_2 was first converted to its oxalate form using suitable amount of oxalic acid and then it was dissolved in millipore water in the presence of nitric acid. Homogeneous mixture solution was stirred up and appropriate amount of citric acid was given. For the gel formation, the extra water was evaporated using a thermal water bath at temperature $80 - 90$ °C. After successful gel formation, it was decomposed at slightly higher temperature (~ 150 °C) and black porous powder was formed. To get the crystalline compound the pelletized powder was annealed at 800 °C for 4 h (for Nano-1) and 1000 °C for 6 h (for Nano-2). To characterize the samples, X-ray diffraction study was performed for powder form of the nanocrystalline samples in Rigaku-TTRAX-III diffractometer. For further characterization of the nanocrystalline samples, Scanning Electron Microscopy (SEM) study was carried out. Magnetic Properties of the samples were measured in vibrating sample magnetometer (VSM) equipped with Superconducting Quantum Interference Device (SQUID-VSM). Electrical transport and magneto-transport measurements were performed in longitudinal geometry (with magnetic field) in Cryogenic magnet setup.

3. Experimental results and discussion

X-ray diffraction measurements of the powder sample of the nanoparticles indicate that the compounds has formed in single phase in nature. No detectable impurity was found in X-ray diffraction patterns of Nano-1 and Nano-2 samples. To find out the lattice parameters of the nanocrystalline compounds, the profile fitting was done by Rietveld refinement technique considering 'pbnm' space group symmetry as reported earlier [23]. Extracted lattice parameters for Nano-1 is $a = 5.386 (\pm 0.001)$ Å, $b = 5.384 (\pm 0.001)$ Å, $c = 7.616 (\pm 0.001)$ Å and that for Nano-2 is $a = 5.389 (\pm 0.008)$ Å, $b = 5.386 (\pm 0.002)$ Å, $c = 7.619 (\pm 0.002)$ Å. Experimental X-ray diffraction pattern along with fitted line (red color) and expected Bragg's positions are given in Fig. 1(a). The average particle size was estimated by using Scherrer's formula as described in Ref. [24]. It was found that the average crystalline size for Nano-1 is ~ 38 nm and that for Nano-2 is ~ 56 nm. Additionally, the representative SEM images for the nanocrystalline samples are shown in Fig. 1(b) and (c) (for Nano-2 and

Nano-1 respectively). The estimated average particle size of the nanocrystalline compounds as calculated from the SEM images, agrees quite well with the results extracted from the analysis of XRD spectrums.

As reported earlier, the bulk polycrystalline $\text{Nd}_{0.5}\text{Ca}_{0.5}\text{MnO}_3$ (NCMO) is a charge ordered antiferromagnetic compound having charge ordering transition, $T_{CO} = 250$ K [23]. In our present study we have measured temperature dependent magnetization (M-T) in three different protocols which are Zero Field Cooled Warming (ZFCW), Field Cooled Cooling (FCC), and Field Cooled Warming (FCW). A brief description about the mentioned protocols are given below.

ZFCW: Samples were cooled down in the absence of the external magnetic field. Magnetic field was then applied at the low temperature and magnetization data were recorded during warming from 5 K to 300 K.

FCC: Magnetic field was applied at the room temperature ($T = 300$ K) and magnetization data were recorded during cooling from 300 K to 5 K.

FCW: After the FCC magnetization measurement, magnetization data were recorded again during warming cycle in the presence of the same magnetic field as applied before (FCC).

Magnetization as a function of temperature in the presence of $H = 50$ kOe external magnetic field is given in Fig. 2. In contrast to the reported magnetization behavior by Zhou et al. for NCMO nanoparticles, our study indicates that signature of the charge ordering transition is clearly visible in nanoparticles [22]. Along with the charge ordering, the rapid increase of magnetization is observed below $T = 130$ K. Such increasing magnetization in NCMO nanoparticles is also reported previously [22]. Regarding this context it is important to mention that with the larger value of magnetization, the increasing nature of magnetization appeared for Nano-2 sample at slightly higher temperature compared to Nano-1 sample. To elucidate the nature of the magnetic interaction, we have plotted inverse susceptibility ($1/\chi$) as a function of temperature for both the Nano-1 and Nano-2 samples. The paramagnetic Curie temperature (θ) was determined from the extrapolated linear fitting of $1/\chi$ (T) data in paramagnetic region which is shown in Fig. 3. For bulk compound the Double Exchange (DE) interaction mediated short range ferromagnetic correlation between the Mn^{3+} and Mn^{4+} ions is well familiar [22,25,26]. Generally with reduction of the particle size for charge ordered nanocrystalline compound, the ferromagnetic phase fraction is increased with the suppression of the antiferromagnetic phase [17]. However, the magnetic interaction strength is reduced in both (ferromagnetic and antiferromagnetic) with the reduction of the particle size [22,27]. The modification of the interaction should be influenced in the value of paramagnetic Curie temperature (θ). Such important information about the different magnetic correlation strength can be extracted from the linear fitting of the $1/\chi$ (T) data in paramagnetic region. In case of the NCMO bulk compounds (as reported earlier), the paramagnetic Curie temperature, $\theta = 202$ K [22]. Whereas, in case of nanocrystalline compounds, value of θ is reduced with the reduction of the particle size which is given in Fig. 3.

For more deeper understanding about the modification of the magnetic ground state with the reduction of the particle size in NCMO compounds, we have carried out the isothermal magnetization measurements at $T = 80$ K. For these measurements, samples were cooled down to 80 K in absence of any external magnetic field (ZFC) from the room temperature $T = 300$ K (paramagnetic state) to remove the effect of any previous measurements if present. Magnetic field dependent magnetization data (M(H)) indicates that with increasing magnetic field, the charge ordered antiferromagnetic phase fraction gets melted in both the nanoparticles and resulting the hysteresis loop at high magnetic field as shown in the main panel of Fig. 4. Additionally, the nature of ferromagnetic ground state was also found and depicted in the upper inset of the Fig. 4. As described earlier, the ferromagnetic interaction is larger in Nano-2 sample compared to the Nano-1 sample. Influence of this modification of the interaction should reflect in their

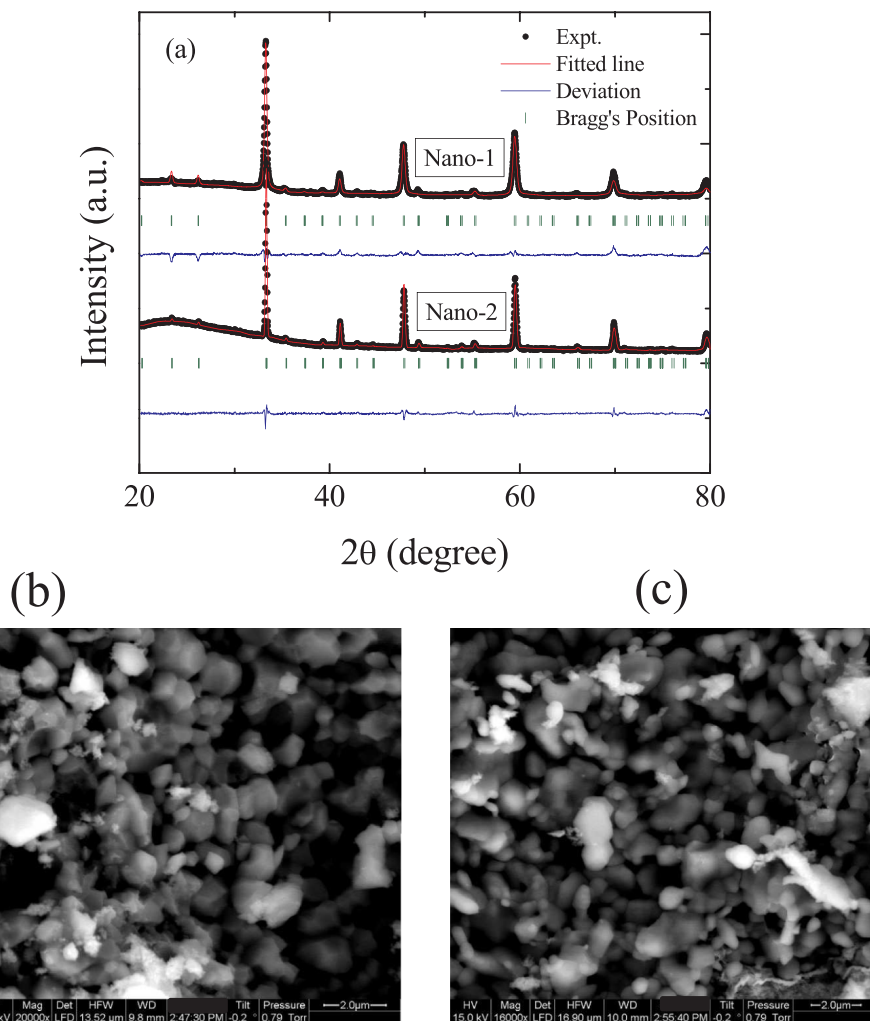


Fig. 1. (a) Room temperature X-ray diffraction patterns along with the profile fitting (red lines) for $\text{Nd}_{0.5}\text{Ca}_{0.5}\text{MnO}_3$ nanocrystalline compounds. (b) and (c) represents the scanning electron microscopy (SEM) image of Nano-2 and Nano-1 samples respectively.

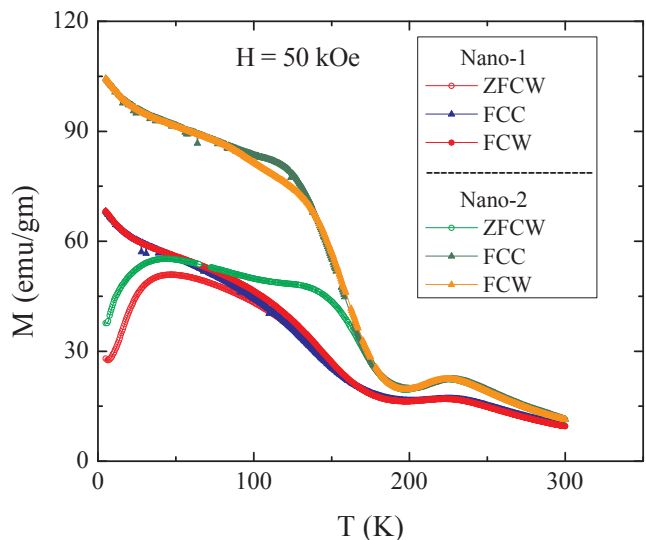


Fig. 2. Magnetization as a function of temperature in the presence of $H = 50$ kOe external magnetic field in different protocols (discussed in the text).

field dependent magnetization ($M(H)$). Derivative of first quadrant magnetization (with respect to magnetic field, dM/dH) as a function of magnetic field (shown in lower inset of Fig. 4.) indicates that the

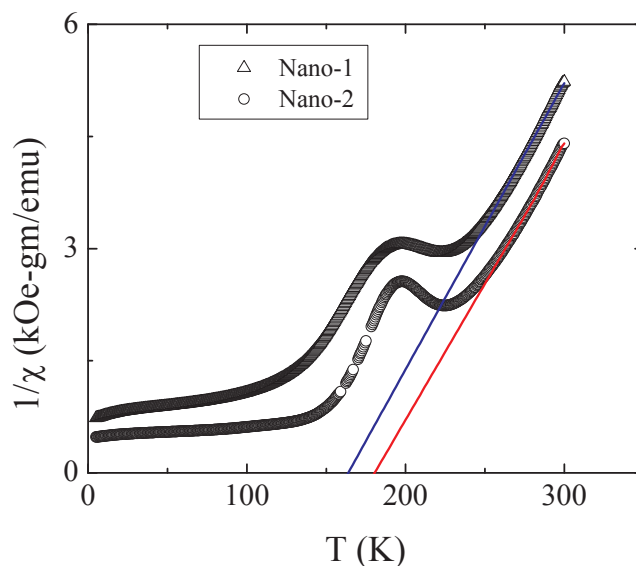


Fig. 3. Temperature dependence of inverse susceptibility of the nanocrystalline compounds. Red and blue lines are the extrapolated linear fitting of the experimental data in the paramagnetic region.

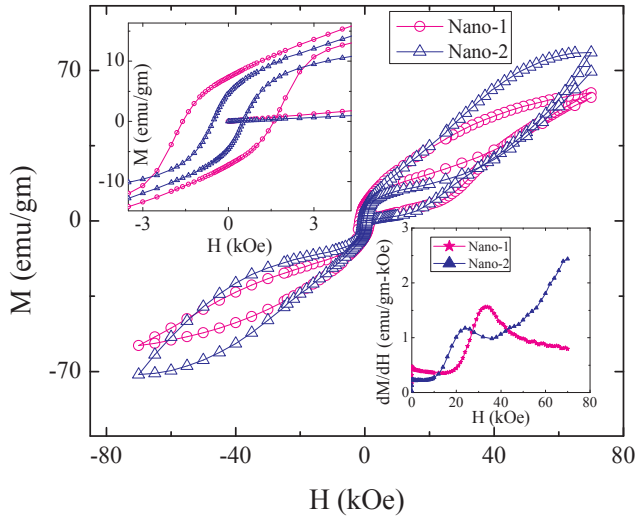


Fig. 4. External magnetic field dependent magnetization of $\text{Nd}_{0.5}\text{Ca}_{0.5}\text{MnO}_3$ nanocrystalline compounds at $T = 80$ K. Upper inset is the enlarged view at the low field region. Lower inset is the derivative of magnetization (with respect to magnetic field) as a function of field.

required critical field is smaller for Nano-2 sample compared to that of Nano-1. As the electronic transport and magneto-transport properties of strongly correlated system are noticeably influenced by the different kind of the exchange interactions, henceforth it is expected to acquire modified magneto-transport properties for the studied samples (Nano-1 and Nano-2).

Resistance as a function of temperature in the absence and in the presence of external magnetic field of 70 kOe for the both samples were measured during cooling and warming cycles. In the absence of magnetic field, both samples exhibit insulating nature with decreasing temperature. This is an almost generic nature of the charge ordered

antiferromagnetic compounds. However, in the presence of the 70 kOe external magnetic field, an insulator-metal transition appears which is shown in Fig. 4 and Fig. 5(b). The insulator-metal transition temperature (TMI) for Nano-1 and Nano-2 is 152 K and 168 K respectively. The experimental results pointing out the direct reflection of the enhanced double exchange interaction in Nano-2 sample which corroborates the metal-insulator transition at higher temperature compared to Nano-1 sample.

The Magnetoresistance of the two samples were calculated from the conservative definition. Magnetoresistance (MR) is the change of electrical resistance of materials when it is subjected in an external magnetic field. MR is quantified by the mathematical expression given below

$$MR\% = \frac{R(H) - R(0)}{R(0)} \times 100 \quad (1)$$

Temperature dependence of MR at $H = 70$ kOe external magnetic field is given in Fig. 5(c). The large magnetoresistance was observed in both the samples at the low temperatures especially below 150 K. Above this temperature the MR values of Nano-1 is larger compared to the Nano-2 sample.

From the technological perspectives, appearance of large magnetoresistance in comparatively smaller value of external magnetic field is one of the important criteria. For the charge ordered antiferromagnetic manganite materials (magnetization and magneto-transport properties are correlated), generally large MR appears at very high magnetic field due to the melting of the antiferromagnetic ground state [15]. Reduction of the particle size inhibits the ferromagnetic phase fraction and influences the magnetoresistance significantly [16]. However, in this study, our experimental results indicate that along with the ferromagnetic phase fraction, the developed interaction (ferromagnetic) also influence its magnetoresistive properties. We have calculated the field dependent magnetoresistance of the Nano-1 and Nano-2 samples at $T = 80$ K which is shown in Fig. 6. The nature of magnetoresistance indicates that the critical field requirement for the lowest particle size

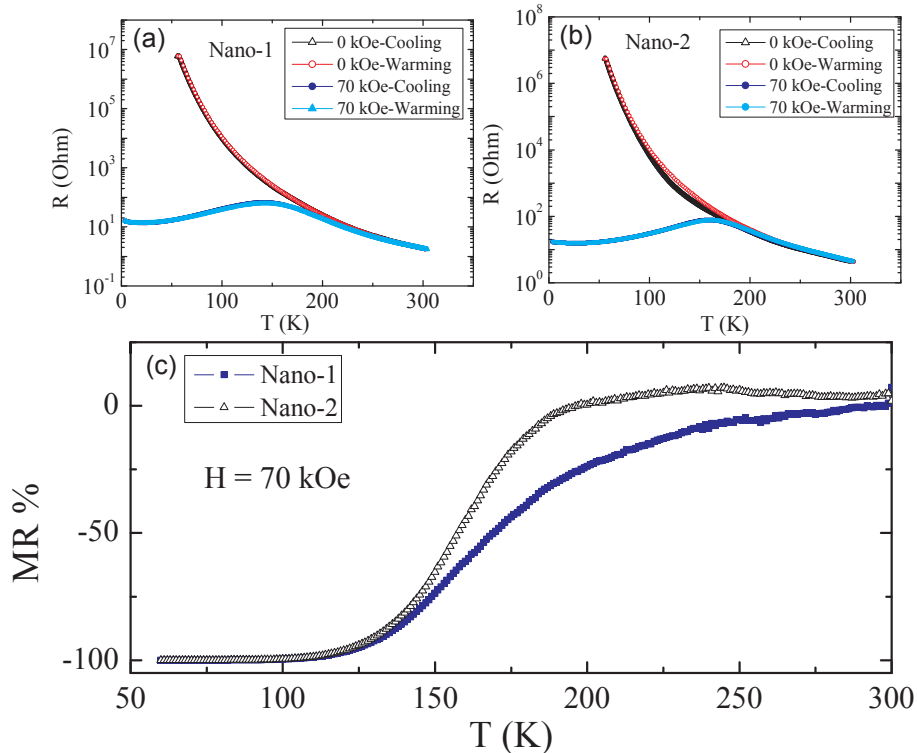


Fig. 5. Temperature dependent resistance (during cooling and warming) in the presence of different external magnetic fields for (a) Nano-1 and (b) Nano-2. (c) Magnetoresistance as a function of temperature of Nano-1 and Nano-2 samples in the presence of $H = 70$ kOe external magnetic field.

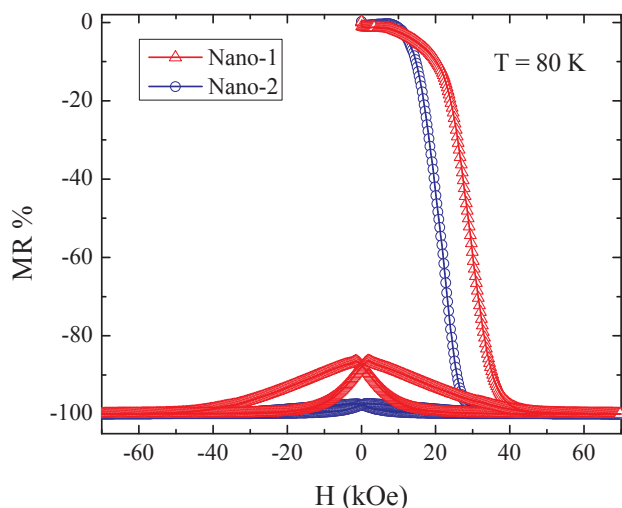


Fig. 6. Magnetoresistance as a function of external magnetic fields at $T = 80$ K for $\text{Nd}_{0.5}\text{Ca}_{0.5}\text{MnO}_3$ nanocrystalline compound.

sample Nano-1 is large compared to that of Nano-2 sample as similar to $M(H)$ behavior and resulting in the large magnetoresistance. Regarding this context, it is worth mentioning that except the ferromagnetic interaction, pinning centres, local disorder etc. might be associated for the higher value of the critical field in case of the Nano-1 sample (lower particle size).

For verification of such phenomenology, we have carried out magneto-transport measurement again at $H = 0$ and 30 kOe external magnetic field. Additionally, the magnetoresistance as a function of temperature have been calculated for 30 kOe magnetic field. All results are plotted in Fig. 7. For Nano-1 sample, quantitative values of resistance reduced at low temperature due to presence of external

magnetic field but insulator to metal transition is hindered (shown in Fig. 7(a)). In contrast to that, different nature was found in case of Nano-2 sample. In the presence of external magnetic field (30 kOe), insulator to metal transition take place at $T = 130$ K (Fig. 7(b)). Such nature again indicates that the ferromagnetic correlation might be stronger in Nano-2 sample than in Nano-1. The variation of calculated magnetoresistance with temperature for two samples is given in Fig. 7(c). Interestingly, the opposite nature was found compared to the magnetoresistance variation in the presence of 70 kOe magnetic field (as shown in Fig. 5(c)). In the presence of the 70 kOe external magnetic field, the MR values were larger in case of the Nano-1 sample. In contrast to that, at the presence of 30 kOe external magnetic field, a crossover was found at $T = 150$ K and MR reaches larger values for Nano-2 sample at low temperature region. Such exotic responses of the nanoparticles has been addressed schematically in Fig. 8.

At very small magnetic field or in the absence of magnetic field charge ordered antiferromagnetic core along with short range ferromagnetically disordered shell are exist in both the nanoparticles. However, in the presence of external magnetic field, spin alignment appears along the magnetic field direction in the shell part and also the core volume get reduced. According to our concerned experimental results, the ferromagnetic interaction is larger in Nano-2 sample compared to Nano-1. In our schematic diagram such spin-spin interaction is addressed by the line having different thickness. Such spin alignments with strong spin-spin correlation (middle column of Fig. 8) in Nano-2 sample, modifies magnetoresistive properties drastically and governs large magnetoresistance compared to Nano-1 sample at medium magnetic field ($H = 30$ kOe). In contrast to that at higher value of the magnetic field, ferromagnetic volume fraction in Nano-1 sample is larger compared to the Nano-2 sample (core part may be totally suppressed in Nano-1 sample) and resulting larger magnetoresistance.

4. Conclusions

To summarize, we have carried out the magnetic and magneto-

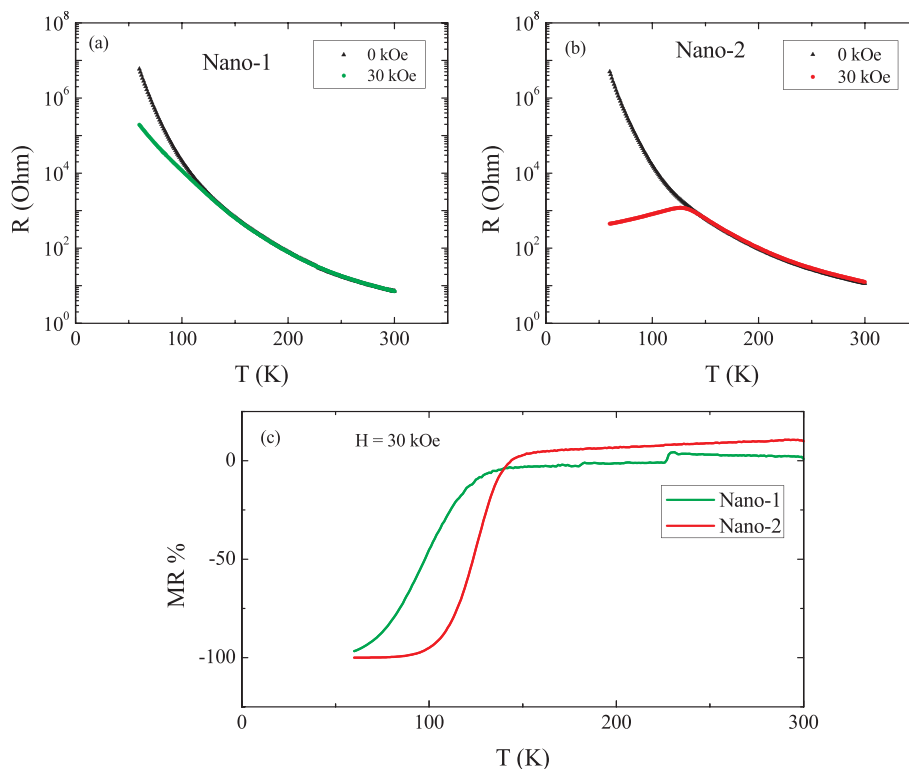


Fig. 7. Temperature dependent resistance (during cooling and warming) in the presence of different external magnetic field for (a) Nano-1 and (b) Nano-2. (c) Magnetoresistance as a function of temperature of Nano-1 and Nano-2 samples in the presence of $H = 30$ kOe external magnetic field.

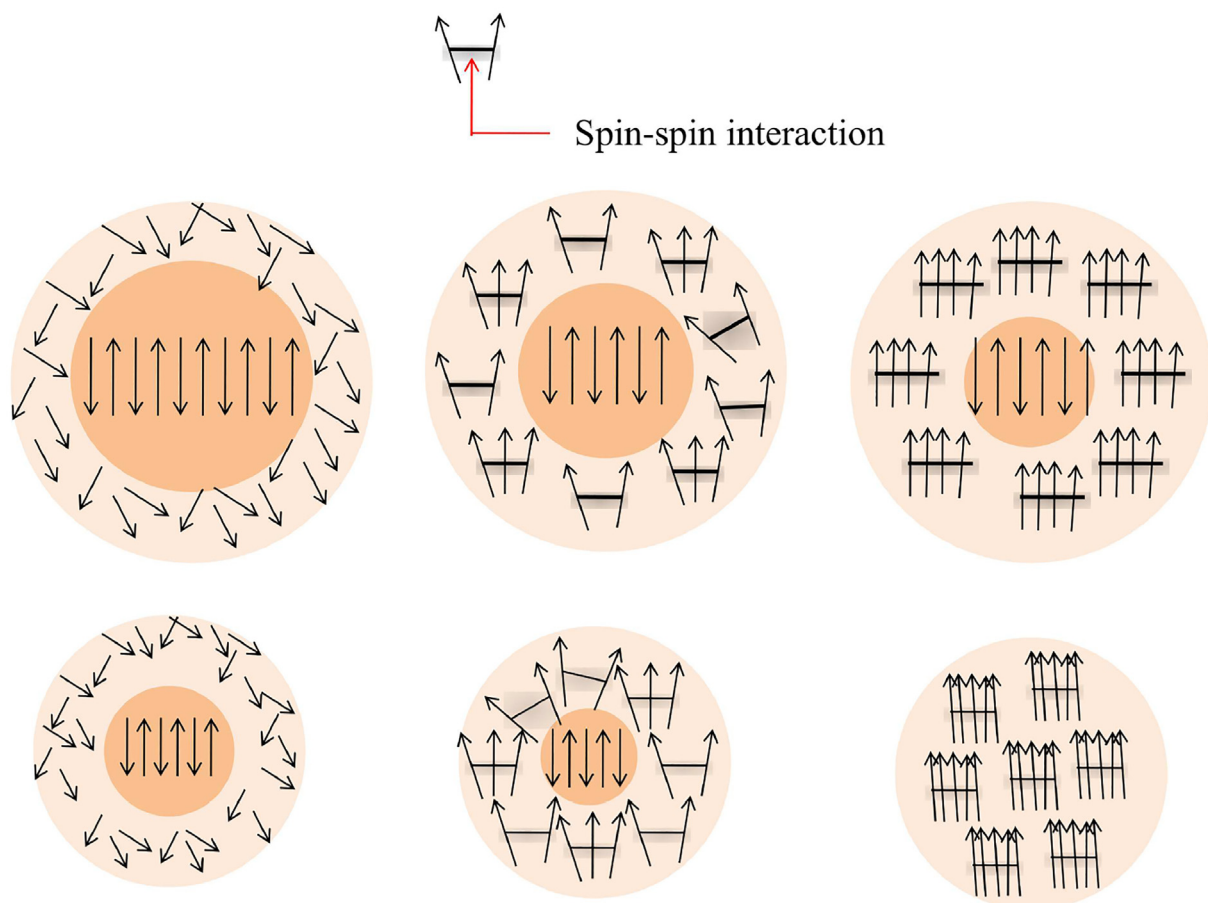


Fig. 8. Schematic representation of spin configuration of nanoparticles. Lower and upper panels are for Nano-1 and Nano-2 sample respectively. Extreme left column is at very small external magnetic field, middle is at the medium and extreme right is at higher value of external magnetic field (along upward direction). Thick joining line between the spins in Nano-2 sample represents strong nature of the interaction strength compared to Nano-1 sample (thin joining line between spins).

transport measurements of NCMO nanocrystalline compounds. Due to the particle size reduction, in contrast to the bulk counterparts, the predominant ferromagnetism appears. However, with the modification of the ferromagnetic volume fractions, the interaction strength also modified with particle size. Such modification of the interaction in nanocrystalline compounds plays the crucial role in magneto-transport and magnetoresistive properties. Additionally, from the technological aspects, the large magnetoresistance in Nano-2 sample may be useful for the several application perspectives.

Declaration of Competing Interest

The authors declare that they have no known competing financial interests or personal relationships that could have appeared to influence the work reported in this paper.

Acknowledgement

The work was supported by Department of Atomic Energy (DAE), Govt. of India.

References

- [1] Colossal Magnetoresistive Oxides, edited by Y. Tokura (Gordon and Breach Science, Amsterdam, 2000).
- [2] H. Kuwahara, Y. Tomioka, A. Asamitsu, Y. Morimoto, Y. Tokura, *Science* 270 (1995) 961.
- [3] A. Biswas, I. Das, C. Majumdar, *J. Appl. Phys.* 98 (2005) 124310.
- [4] A. Biswas, I. Das, *Phys. Rev. B* 74 (2006) 172405.
- [5] A. Biswas, S. Tapas Samanta, S. Banerjee, I. Das, *Phys. Lett.* 94 (2009) 233109.
- [6] A. Biswas, I. Das, *J. Appl. Phys.* 102 (2007) 064303.
- [7] A. Biswas, I. Das, *Appl. Phys. Lett.* 92 (2008) 012502.
- [8] M. Uehara, S. Mori, C.H. Chen, S.-W. Cheong, *Nature (London)* 399 (1999) 560.
- [9] L. Zhang, C. Israel, A. Biswas, R.L. Greene, A. de Lozanne, *Science* 298 (2002) 805.
- [10] S. Dong, R. Yu, S. Yunoki, J.-M. Liu, E. Dagotto, *Phys. Rev. B* 78 (2008) 064414.
- [11] K. Das, R. Rawat, B. Satpati, I. Das, *Appl. Phys. Lett.* 103 (2013) 202406.
- [12] K. Das, B. Satpati, I. Das, *RSC Adv.* 5 (2015) 27338.
- [13] S. Jin, T.H. Tiefel, M. McCormack, R.A. Fastnacht, R. Ramesh, L.H. Chen, *Science* 264 (1994) 413.
- [14] A. Biswas, T. Samanta, S. Banerjee, I. Das, *Appl. Phys. Lett.* 92 (2008) 012502.
- [15] Y. Tokura, *Rep. Prog. Phys.* 69 (2006) 797.
- [16] K. Das, P. Dasgupta, A. Poddar, I. Das, *Sci. Rep.* 6 (2016) 20351.
- [17] S. Dong, F. Gao, Z.Q. Wang, J.-M. Liu, *Appl. Phys. Lett.* 90 (2007) 082508.
- [18] K. Das, I. Das, *J. Appl. Phys.* 119 (2016) 093903.
- [19] M.H. Phan, S. Chandra, N.S. Bingham, H. Srikanth, C.L. Zhang, S.W. Cheong, T.D. Hoang, H.D. Chinh, *Appl. Phys. Lett.* 97 (2010) 242506.
- [20] T. Sarkar, B. Ghosh, A.K. Raychaudhuri, T. Chatterji, *Phys. Rev. B* 77 (2008) 235112.
- [21] T. Zhang, T.F. Zhou, T. Qian, X.G. Li, *Phys. Rev. B* 76 (2007) 174415.
- [22] S. Zhou, Y. Guo, C. Wang, L. He, J. Zhao, L. Shi, *Dalton Trans.* 41 (2012) 7109.
- [23] T. Vogt, A.K. Cheetham, R. Mahendiran, A.K. Raychaudhuri, R. Mahesh, C.N.R. Rao, *Phys. Rev. B* 54 (1996) 15303.
- [24] K. Das, I. Das, *J. Appl. Phys.* 118 (2015) 084302.
- [25] W. Bao, J.D. Axe, C.H. Chen, S.-W. Cheong, *Phys. Rev. Lett.* 78 (1997) 543.
- [26] A. Daoud-Aladine, L. Pinsard-Gaudart, M.T. Fernandez-Daz, A. Revcolevschi, *Phys. Rev. Lett.* 89 (2002) 097205.
- [27] S. Zhou, Y. Guo, J. Zhao, L. He, C. Wang, L. Shi, *J. Phys. Chem. C* 115 (2011) 11500–11506.